

Photon radiation in $e^+e^- \rightarrow \text{hadrons}$ at low energies with carlomat_3.1

Karol Kołodziej

Institute of Physics
University of Silesia
Katowice, Poland

First Workshop of the Muon $g-2$ Theory Initiative

Fermilab, 3-6 June 2017

Motivation

The hadronic contribution to vacuum polarization can be derived, with the help of dispersion relations, from the energy dependence of the ratio

$$R_\gamma(s) \equiv \sigma^{(0)}(e^+e^- \rightarrow \gamma^* \rightarrow \text{hadrons}) / \frac{4\pi\alpha^2}{3s}$$

One of the main issues is $R_\gamma(s)$ in the region from 1.2 to 2.0 GeV, where more than 30 exclusive channels must be measured.

To obtain reliable theoretical predictions for that many hadronic processes is a challenge indeed.

It is obvious that the correct description of the most relevant hadronic channels as, e.g., $\pi^+\pi^-$, requires the inclusion of radiative corrections. This demand is met e.g. by the dedicated Monte Carlo (MC) generator PHOKHARA.

Motivation

However, it is probably enough to have the leading order (LO) predictions for many sub-dominant channels, with three or more particles in the final state.

If those channels are measured with the method of radiative return, as is done by KLOE, BaBar and BES, the predictions must also include radiation of photons, both from the initial (ISR) and final (FSR) state.

Production of hadrons at low energies, as well as the photon radiation off them, is usually described in the framework of some effective model which often includes quite a number of interaction vertices and mixing terms.

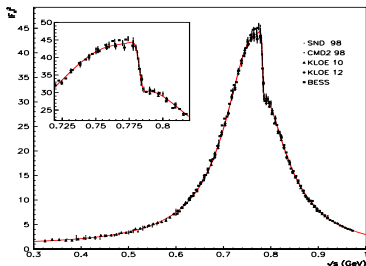
⇒ # Feynman diagrams of such sub-dominant multiparticle processes may become quite big.

⇒ There is a strong need for full automation of the MC code generation.

Motivation

A promising theoretical framework for the description of $e^+e^- \rightarrow \text{hadrons}$ at low energies is the Hidden Local Symmetry (HLS) model.

The HLS model, supplemented by isospin and SU(3) breaking effects, works surprisingly well up to 1.05 GeV, just including the ϕ meson.



The global HLS model fit of the $\pi\pi$ channel together with the data from Novosibirsk, Frascati and Beijing

[M. Benayoun, et al. EPJ C]

Motivation

MC programs for description of processes $e^+e^- \rightarrow$ hadrons at low centre of mass energies can be generated automatically with program `carlomat_3.0`. [K. Kołodziej, CPC 196 (2015) 563]

The program

- incorporates a photon–vector meson mixing,
- includes the Feynman interaction vertices of HLS model and the effective Lagrangian of the EM interaction of nucleons,
- introduces new options to enable a better control over the effective models implemented.

Motivation

MC programs for description of processes $e^+e^- \rightarrow$ hadrons at low centre of mass energies can be generated automatically with program `carlomat_3.0`. [K. Kołodziej, CPC 196 (2015) 563]

The program

- incorporates a photon–vector meson mixing,
- includes the Feynman interaction vertices of HLS model and the effective Lagrangian of the EM interaction of nucleons,
- introduces new options to enable a better control over the effective models implemented.

`carlomat_3.1` offers a possibility of

- taking into account either the ISR or FSR separately, or both at a time,
- inclusion of the EM charged pion form factor for processes with charged pion pairs,
- the $U(1)$ EM gauge invariance tests.

Motivation

MC programs for description of processes $e^+e^- \rightarrow$ hadrons at low centre of mass energies can be generated automatically with program [carlomat_3.0](#). [K. Kołodziej, CPC 196 (2015) 563]

The program


- incorporates a photon–vector meson mixing,
- includes the Feynman interaction vertices of HLS model and the effective Lagrangian of the EM interaction of nucleons,
- introduces new options to enable a better control over the effective models implemented.

[carlomat_3.1](#) offers a possibility of

- taking into account either the ISR or FSR separately, or both at a time,
- inclusion of the EM charged pion form factor for processes with charged pion pairs,
- the $U(1)$ EM gauge invariance tests.

q^2 -dependent mixing terms

In spite of being conceptually quite simple, the implementation of particle mixing required substantial changes in the code generation part of the program.


$$A^\mu(q) \quad V^\nu(q) \quad \equiv \quad -ef_{AV}(q^2) g^{\mu\nu},$$


with $V = \rho^0, \omega, \phi, \rho_1 = \rho(1450), \rho_2 = \rho(1700)$.

The mixing term introduces an extra power of $e \Rightarrow$ it should be included only once in a Feynman diagram.

q^2 -dependent mixing terms

In spite of being conceptually quite simple, the implementation of particle mixing required substantial changes in the code generation part of the program.

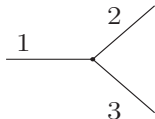
$$A^\mu(q) \quad V^\nu(q) \quad \equiv \quad -ef_{AV}(q^2) g^{\mu\nu},$$


with $V = \rho^0, \omega, \phi, \rho_1 = \rho(1450), \rho_2 = \rho(1700)$.

The mixing term introduces an extra power of $e \Rightarrow$ it should be included only once in a Feynman diagram.

Topology generation in carlomat

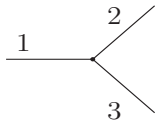
Topologies are generated for models with **triple** and **quartic** couplings, starting with **1 topology** of a **3 particle** process.



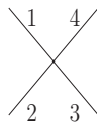
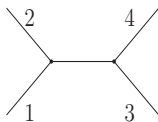
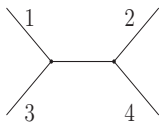
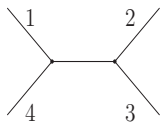
Line 4 is attached to **each line** and to **the vertex** \Rightarrow **4 topologies** of a **4 particle** process.

Topology generation in carlomat

Topologies are generated for models with **triple** and **quartic** couplings, starting with **1 topology** of a **3 particle** process.

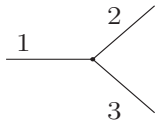


Line 4 is attached to **each line** and to **the vertex** \Rightarrow **4 topologies** of a **4 particle** process.

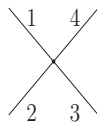
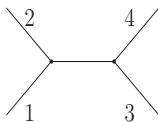
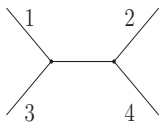
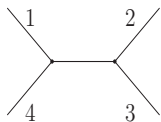


Topology generation in carlomat

Topologies are generated for models with **triple** and **quartic** couplings, starting with **1 topology** of a **3 particle** process.



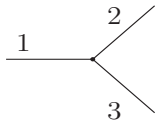
Line 4 is attached to **each line** and to **the vertex** \Rightarrow **4 topologies** of a **4 particle** process.



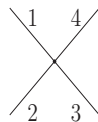
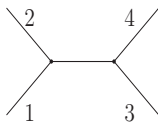
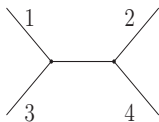
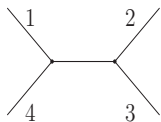
Line 5 is attached to **each line**, including the internal ones, and to each **triple vertex** \Rightarrow **25 topologies** of a **5 particle** process.

Topology generation in carlomat

Topologies are generated for models with **triple** and **quartic** couplings, starting with **1 topology** of a **3 particle** process.



Line 4 is attached to **each line** and to **the vertex** \Rightarrow **4 topologies** of a **4 particle** process.



Line 5 is attached to **each line**, including the internal ones, and to each **triple vertex** \Rightarrow **25 topologies** of a **5 particle** process.

Topology generation in carlomat

of topologies grows dramatically with # of external particles.

# of particles	# of topologies
6	220
7	2 485
8	34 300
9	559 405
10	10 525 900
11	224 449 225

n external particles \Rightarrow topologies for $n - 1$ particles needed

Topology generation in carlomat

of topologies grows dramatically with # of external particles.

# of particles	# of topologies
6	220
7	2 485
8	34 300
9	559 405
10	10 525 900
11	224 449 225

n external particles \Rightarrow topologies for $n - 1$ particles needed
 \Rightarrow Feynman rules checked while adding the n -th particle.

Topology generation in carlomat

of topologies grows dramatically with # of external particles.

# of particles	# of topologies
6	220
7	2 485
8	34 300
9	559 405
10	10 525 900
11	224 449 225

n external particles \Rightarrow topologies for $n - 1$ particles needed
 \Rightarrow Feynman rules checked while adding the n -th particle.

To facilitate this, each topology is divided into two parts, each being checked against the Feynman rules separately.

Topology generation in carlomat

of topologies grows dramatically with # of external particles.

# of particles	# of topologies
6	220
7	2 485
8	34 300
9	559 405
10	10 525 900
11	224 449 225

n external particles \Rightarrow topologies for $n - 1$ particles needed
 \Rightarrow Feynman rules checked while adding the n -th particle.

To facilitate this, each topology is divided into two parts, each being checked against the Feynman rules separately.

The particle mixing is added just at this stage.

Topology generation in carlomat

of topologies grows dramatically with # of external particles.

# of particles	# of topologies
6	220
7	2 485
8	34 300
9	559 405
10	10 525 900
11	224 449 225

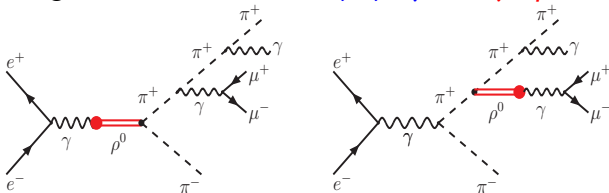
n external particles \Rightarrow topologies for $n-1$ particles needed
 \Rightarrow Feynman rules checked while adding the n -th particle.

To facilitate this, each topology is divided into two parts, each being checked against the Feynman rules separately.

The particle mixing is added just at this stage.

q^2 -dependent mixing terms - example

Feynman diagrams of $e^+e^- \rightarrow \pi^+\pi^-\mu^+\mu^-\gamma$ with $\gamma-\rho^0$ mixing:

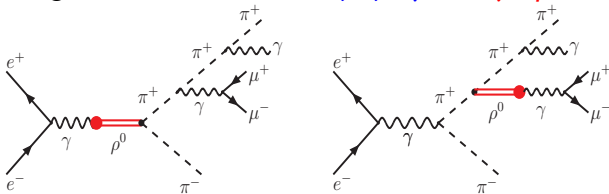


Two (three) particles are combined into the third (fourth) leg of a triple (quartic) Feynman vertex which is then folded with the adjacent Feynman propagator to form an off shell particle.

That is represented by an array of spinors, polarization vectors or scalars, with elements labelled with the polarization indices of spinors or polarization vectors of which it is formed.

q^2 -dependent mixing terms - example

Feynman diagrams of $e^+e^- \rightarrow \pi^+\pi^-\mu^+\mu^-\gamma$ with $\gamma-\rho^0$ mixing:



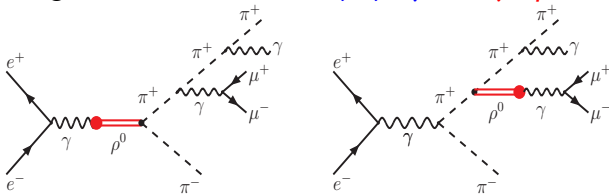
Two (three) particles are combined into the third (fourth) leg of a triple (quartic) Feynman vertex which is then folded with the adjacent Feynman propagator to form an off shell particle.

That is represented by an array of spinors, polarization vectors or scalars, with elements labelled with the polarization indices of spinors or polarization vectors of which it is formed.

If the particle mixing is present, the program checks whether the propagator of the off shell particle can be mixed or not, if so, a new off shell particle is formed.

q^2 -dependent mixing terms - example

Feynman diagrams of $e^+e^- \rightarrow \pi^+\pi^-\mu^+\mu^-\gamma$ with $\gamma-\rho^0$ mixing:



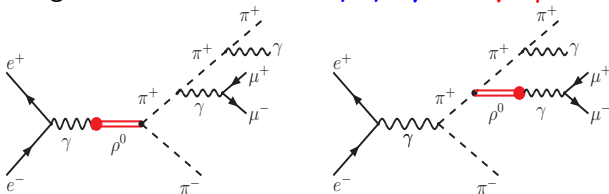
Two (three) particles are combined into the third (fourth) leg of a triple (quartic) Feynman vertex which is then folded with the adjacent Feynman propagator to form an off shell particle.

That is represented by an array of spinors, polarization vectors or scalars, with elements labelled with the polarization indices of spinors or polarization vectors of which it is formed.

If the particle mixing is present, the program checks whether the propagator of the off shell particle can be mixed or not, if so, a new off shell particle is formed. The particle with mixing is appropriately tagged in order not to be mixed again.

q^2 -dependent mixing terms - example

Feynman diagrams of $e^+e^- \rightarrow \pi^+\pi^-\mu^+\mu^-\gamma$ with $\gamma-\rho^0$ mixing:



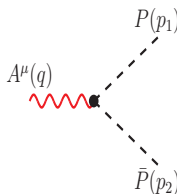
Two (three) particles are combined into the third (fourth) leg of a triple (quartic) Feynman vertex which is then folded with the adjacent Feynman propagator to form an off shell particle.

That is represented by an array of spinors, polarization vectors or scalars, with elements labelled with the polarization indices of spinors or polarization vectors of which it is formed.

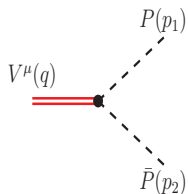
If the particle mixing is present, the program checks whether the propagator of the off shell particle can be mixed or not, if so, a new off shell particle is formed. The particle with mixing is appropriately tagged in order not to be mixed again.

q^2 -dependent interaction vertices

Triple vertices of the form similar to those of sQED:



A Feynman diagram showing a triple vertex. On the left, a wavy red line representing a photon with momentum q and index μ , labeled $A^\mu(q)$, enters from the left. On the right, two dashed lines representing pseudoscalars emerge: one with momentum p_1 and index μ , labeled $P(p_1)$, and another with momentum p_2 and index μ , labeled $\bar{P}(p_2)$. The vertex is a black dot. To the right of the diagram is the expression $\equiv ief_{APP}(q^2)(p_1 - p_2)^\mu$.



A Feynman diagram showing a triple vertex. On the left, a double red line representing a vector meson with momentum q and index μ , labeled $V^\mu(q)$, enters from the left. On the right, two dashed lines representing pseudoscalars emerge: one with momentum p_1 and index μ , labeled $P(p_1)$, and another with momentum p_2 and index μ , labeled $\bar{P}(p_2)$. The vertex is a black dot. To the right of the diagram is the expression $\equiv if_{VPP}(q^2)(p_1 - p_2)^\mu$.

where $V = \rho^0, \omega, \phi$ and $P = \pi^+, K^+, K^0$.

q^2 -dependent interaction vertices

Triple vertices of a more complicated tensor form:

$$\pi^0(q) \equiv e^2 f_{\pi AA}(q^2) \varepsilon^{\mu\nu\alpha\beta} p_{1\alpha} p_{2\beta}$$

$$\pi^0(q) \equiv i e f_{\pi AV}(q^2) \varepsilon^{\mu\nu\alpha\beta} p_{1\alpha} p_{2\beta}$$

$$\pi^\mp(q) \equiv i e f_{\pi^\mp A\rho^\pm}(q^2) \varepsilon^{\mu\nu\alpha\beta} p_{1\alpha} p_{2\beta}$$

$$P(q) \equiv f_{P\omega V}(q^2) \varepsilon^{\mu\nu\alpha\beta} p_{1\alpha} p_{2\beta}$$

where, in the top right corner, $V = \rho^0, \omega$, and in the bottom right corner $P = \pi^0$ and $V = \rho^0$ or $P = \pi^\mp$ and $V = \rho^\pm$.

q^2 -dependent interaction vertices

Quartic vertices of the HLS model:

$$\equiv 2ie f_{A\rho\pi\pi}(q^2)g^{\mu\nu}$$

$$\equiv 2if_{\rho\rho\pi\pi}(q^2)g^{\mu\nu}$$

$$\equiv -ef_{A\pi\pi\pi}(q^2)\varepsilon^{\mu\nu\alpha\beta}p_{1\nu}p_{2\alpha}p_{3\beta}$$

$$\equiv -ef_{\omega\pi\pi\pi}(q^2)\varepsilon^{\mu\nu\alpha\beta}p_{1\nu}p_{2\alpha}p_{3\beta}$$

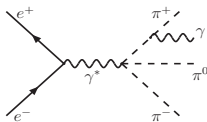
The vertices in the first row have the same tensor form as the quartic vertex of the sQED or the quartic vertices of the Nambu-Goldstone boson – gauge boson interaction of the SM, which were implemented already in the first version of carlomat.

Results for pion production processes

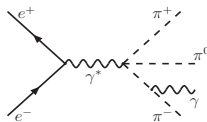
The cross sections in pb at $\sqrt{s} = 1$ GeV and the $U(1)$ gauge invariance tests. Cuts: $E_\gamma > 0.01$ GeV, $5^\circ < \theta_{\gamma\text{beam}} < 175^\circ$. The MC uncertainty of the last digits is shown in parentheses.

Process	ISR			Full LO		
	# diags	σ	$\sigma _{\varepsilon(k)=k}$	# diags	σ	$\sigma _{\varepsilon(k)=k}$
$e^+e^- \rightarrow \pi^+\pi^-\gamma$	2	2.041(4)e+4	1.04(1)e-28	5	2.249(4)e+4	2.73(2)e-28
$\pi^+\pi^-\pi^0\gamma$	32	409(1)	2.21(3)e-30	156	481.5(6)	3.011(1)e-2
$\pi^+\pi^-\mu^+\mu^-\gamma$	26	4.344(9)e-2	4.62(5)e-34	107	6.449(8)e-2	6.42(5)e-34
$\pi^+\pi^-\pi^+\pi^-\gamma$	36	2.029(5)e-3	2.14(3)e-35	200	3.320(5)e-3	3.03(2)e-35
$\pi^+\pi^-\gamma\gamma$	6	1.445(14)e+3	1.22(4)e-29	44	2.131(8)e+3	2.08(3)e-29
$\pi^+\pi^-\mu^+\mu^-\gamma\gamma$	90	1.127(7)e-3	1.16(4)e-35	1272	2.535(8)e-3	9.56(1)e-19
$\pi^+\pi^-\pi^+\pi^-\gamma\gamma$	120	4.68(3)e-5	4.6(1)e-37	2772	1.303(4)e-4	4.969(4)e-15

The Feynman diagrams of $\pi^+\pi^-\pi^0\gamma$ that cause the $U(1)$ gauge invariance violation:



(1)



(2)

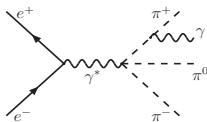
Most probably because a penta vertex $\pi^+\pi^-\pi^0\gamma\gamma$ is missing.

Results for pion production processes

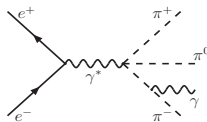
The cross sections in pb at $\sqrt{s} = 1$ GeV and the $U(1)$ gauge invariance tests. Cuts: $E_\gamma > 0.01$ GeV, $5^\circ < \theta_{\gamma\text{beam}} < 175^\circ$. The MC uncertainty of the last digits is shown in parentheses.

Process	ISR			Full LO		
	# diags	σ	$\sigma _{\varepsilon(k)=k}$	# diags	σ	$\sigma _{\varepsilon(k)=k}$
$e^+e^- \rightarrow \pi^+\pi^-\gamma$	2	2.041(4)e+4	1.04(1)e-28	5	2.249(4)e+4	2.73(2)e-28
$\pi^+\pi^-\pi^0\gamma$	32	409(1)	2.21(3)e-30	156	481.5(6)	3.011(1)e-2
$\pi^+\pi^-\mu^+\mu^-\gamma$	26	4.344(9)e-2	4.62(5)e-34	107	6.449(8)e-2	6.42(5)e-34
$\pi^+\pi^-\pi^+\pi^-\gamma$	36	2.029(5)e-3	2.14(3)e-35	200	3.320(5)e-3	3.03(2)e-35
$\pi^+\pi^-\gamma\gamma$	6	1.445(14)e+3	1.22(4)e-29	44	2.131(8)e+3	2.08(3)e-29
$\pi^+\pi^-\mu^+\mu^-\gamma\gamma$	90	1.127(7)e-3	1.16(4)e-35	1272	2.535(8)e-3	9.56(1)e-19
$\pi^+\pi^-\pi^+\pi^-\gamma\gamma$	120	4.68(3)e-5	4.6(1)e-37	2772	1.303(4)e-4	4.969(4)e-15

The Feynman diagrams of $\pi^+\pi^-\pi^0\gamma$ that cause the $U(1)$ gauge invariance violation:



(1)



(2)

Most probably because a penta vertex $\pi^+\pi^-\pi^0\gamma\gamma$ is missing.

Sample results

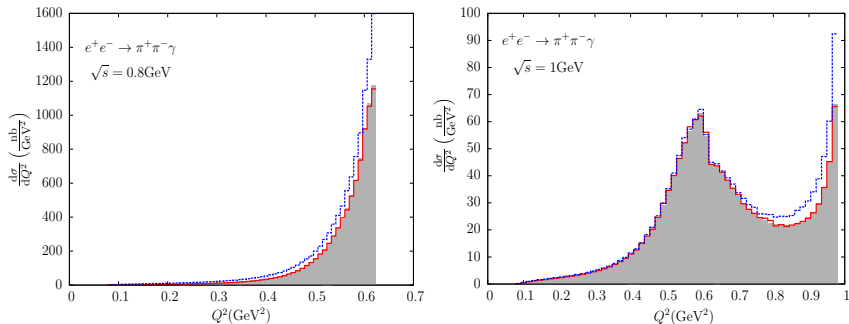


Figure : Differential cross sections of $e^+e^- \rightarrow \pi^+\pi^-\gamma$ as functions of invariant mass of the $\pi^+\pi^-$ -pair, ISR (shaded) and ISR+FSR (dashed)

Analytic result for the differential cross section for radiative events with $\theta_{\min} < \theta < 180^\circ - \theta_{\min}$:

$$Q^2 \frac{d\sigma}{dQ^2} = \frac{4\alpha^3}{3s} R(Q^2) \left[\frac{s^2 + Q^4}{s(s - Q^2)} \log \frac{1 + \cos\theta_{\min}}{1 - \cos\theta_{\min}} - \frac{s - Q^2}{s} \cos\theta_{\min} \right]$$

Sample results

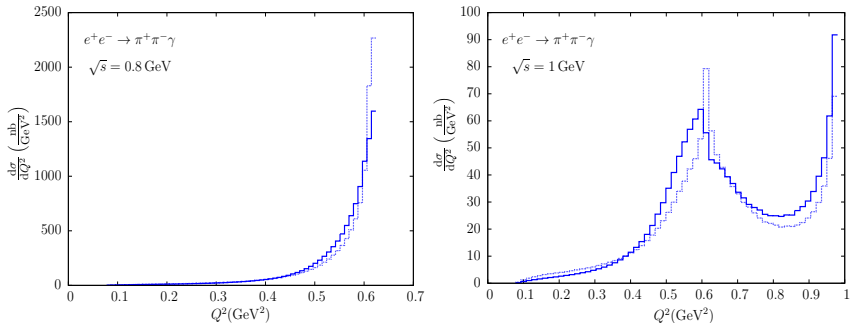


Figure : Differential cross sections of $e^+e^- \rightarrow \pi^+\pi^-\gamma$ as functions of invariant mass of the $\pi^+\pi^-$ -pair computed in a model with the charged pion form factor (*solid lines*) and in the HLS model with fixed couplings (*dotted lines*)

Sample results

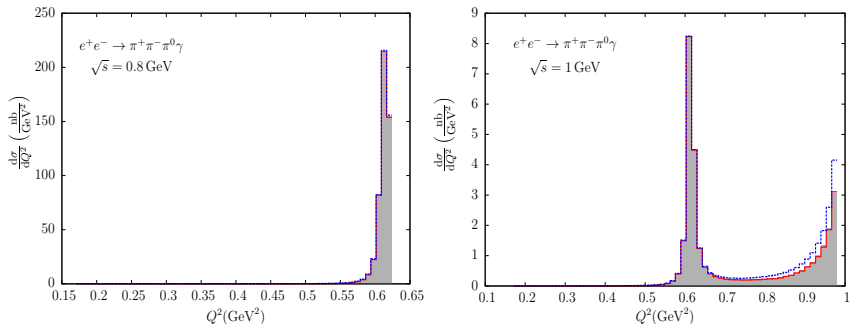


Figure : Differential cross sections of $e^+e^- \rightarrow \pi^+\pi^-\pi^0\gamma$ as functions of invariant mass of the $\pi^+\pi^-\pi^0$ -system

Summary

- `carlomat_3.1` is a new version of a multipurpose program `carlomat` that allows one to generate automatically the MC programs dedicated to the description of, among others, the processes of $e^+e^- \rightarrow \text{hadrons}$ at low centre-of-mass energies.
- The electromagnetic charged pion form factor has been implemented in the program.
- A photon radiation off the initial and final state particles can be taken into account separately, or together.
- The $U(1)$ electromagnetic gauge invariance can be easily tested, which is relevant if the momentum transfer dependence is introduced in the couplings of the HLS model or a set of the couplings implemented in the program is incomplete.
- The program can be controlled at the stage of code generation, by adding or commenting particles, mixing terms and interaction vertices.
- Many options allow to control it at the stage of MC computation, too.

Thank you for your attention